Chapter 17
Analysis of Triple Rectangular Plates Configurations Impacts on Local Scour Around Cylindrical Single Bridge Pier

Alireza Pourzaker Arabani and Hooman Hajikandi

Abstract Triple rectangular plates are used in the experiments on scour around a single cylindrical pier. The tests are carried out under clear water condition. Total 35 runs for three different arrangements of the plates, namely; upstream, downstream and both upstream and downstream configurations, two lengths of the plates and three inflow discharges are conducted. The observations confirmed that the triple plates confined the particle motion and weakened both the horseshoe vortex and the lee wake. In upstream configuration runs, the scoured particles due to the downward jet pileup again near the pier nose, resulting shallower scour depth. Furthermore, the side wall plates resist the sediment movement to the downstream; respectively, in downstream configuration runs the lee-wake is suppressed remarkably. The observations indicate that both the upstream and downstream configurations are jointly effective in restraining the horse shoe vortex. Hence, these innovative scour countermeasures act as bed armoring and flow altering devices, simultaneously. A maximum scour depth reduction efficacy of 62% is achieved for the best arrangement (both upstream and downstream configuration) within the limit of present work. The proposed setup is found to be successful in suppressing the vortices near the pier wall. Furthermore, the longer plates provide more prevention against scour.

Keywords Bottom erosion · Single pier protection · Sedimentation · Scour countermeasures

17.1 Introduction

Bridge pier scour is really a destructive event in river flood scenarios. Kandasamy and Melviell in a research in 1998 have reported that about 60% of bridge failures occurred in New Zealand resulted from abutment scour [1]. The federal highway

A. Pourzaker Arabani (✉) · H. Hajikandi
Euro-HydroInformatics and Water Management, BTU Cottbus University, Cottbus, Germany
e-mail: a.pourzaker@gmail.com

H. Hajikandi
e-mail: Hoo.Haji_kandi@iauctb.ac.ir

P. Gourbesville and G. Caignaert (eds.), *Advances in Hydroinformatics*, Springer Water,
https://doi.org/10.1007/978-981-19-1600-7_17

administration (FHWA) has expressed that among 383 bridge failure cases due to flood in the United States, 25% involved pier damage and 72% were involved abutment damage. Due to the importance of the topic, many researchers have been interested in it during last decades.

The mechanism of scour is very complicated. Numerous studies have been devoted to the investigation of flow pattern around piers [2].

Scour countermeasure devices are classified into two distinct groups, namely flow altering and bed-armoring countermeasures. Flow altering countermeasures include devices attached to the pier or bed, openings through piers or other kinds of innovative devices which are used to change the flow pattern at the vicinity of the pier in such a way to reduce the down flow and horse shoe vortex, which are the main causes of pier scour [3]; Chew and Lim 2003). Bed armoring counter measures include materials and methodologies implemented to increase the shear resistance of the bed around the pier. These materials include ripraps, sand bags or heavy gabion like blocks which are dumped on the bed. Tafarojnorus et al. (2010) have reported a detailed review on flow altering countermeasures. Plates or vanes are used as pier attached countermeasures. Ghorbani and Kells [4] have expressed that pier attached vanes are effective in reducing horse-shoe vortex strength. The earliest use of pier attached vanes as scour countermeasure turns back to Maza et al. [5]. He used two inclined horizontal plates attached respectively to the upstream and downstream faces of the pier with a 1:3 slope. He reported that his suggested configuration was able to provide 70 to 80 percent scour reduction efficiency. Gupta and Gangadharaiah [6] introduced delta wing shaped vanes attached to the pier and showed that a maximum scour depth reduction of 67% under clear water condition is achieved. Gupta and Gangadharaiah [6] reported a minimum 32% scour depth reduction for the aforementioned configuration under live bed condition. Diado [7] studied the performance of slanting plates as well as a guide wall attached to the pier nose, as scour countermeasure and reported 90 percent efficacy in maximum scour depth reduction. Later, Parker et al. [3] tested the configuration proposed by Diado and Yano (1995) in live bed condition and expressed that its efficiency was 50%.

A number of previous studies were devoted to the application of vanes and plates in the form of bed attachment devices. These countermeasures divert the approach flow and weaken the down flow and horse shoe vortex. Submerged vanes, as introduced by [8] are the most popular devices of this category. They generate secondary currents that modify the velocity distribution and reduce the scour rate. Different arrangements of the bed attached vanes and their geometrical length scales were investigated by Lauchlan [9].

17.2 Experiments and Methods

The performance of pier attached plates, under three different configurations as scour countermeasures, is investigated. The plates are made of galvanized iron with 1 mm thickness. Figure 17.1a shows different configurations of the plates used in the tests.

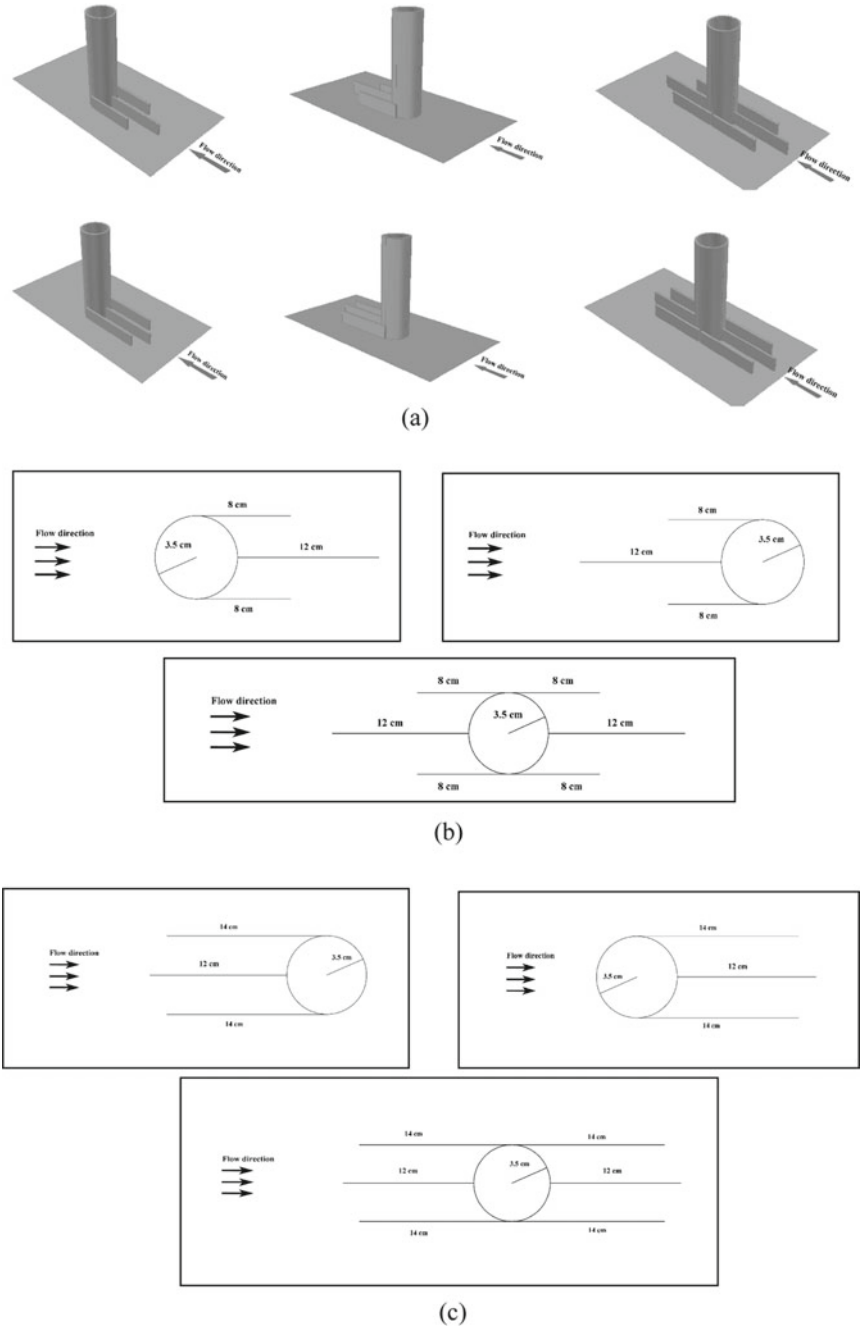

Fig. 17.1 Schematic of the present countermeasures: **a** different configurations, **b** and **c** plates dimensions used in the experiments

In addition, three configurations namely; upstream plates (type 1), downstream plates (type 2) and both upstream and downstream plates (type 3) are considered. For all the cases the plates are installed vertically in flow aligned direction. The heights of the plates were 12 cm, 4 cm of which was embedded into the sediment layer and the remaining 8 cm was exposed to the ambient flow. The length of the middle plates attached to the pier nose (both in upstream and downstream configurations) was fixed to12 cm while two different lengths of 8 cm and 14 cm were used for the lateral plates (see Figs. 17.1b, c).

The experiments were carried out in a towing flume, 10 m long, 1 m wide and 0.8 m deep. The pier was made of PVC with nominal diameter of 7 cm which satisfied the limiting condition of $b/d_p > 10$ (where b is the channel width and d_p is the pier diameter) suggested by Chiew and Melvill [10] to avoid the side effects of the lateral walls on scour pattern. A 2 m long and 20 cm thick sediment recess was located in the middle of the flume which was filled with Sand particles of a median size (d_p) of 0.8 mm and a geometric standard deviation of $\sigma_g = 1.2$. The σ_g of sediment size distribution given by ($\frac{d_{84}}{d_{16}}$) is less than 1.4 in uniformly graded sediments (Breusers and Raudkivi 1991).

Meanwhile the ratio d_p/d_{50} is 87.5 which is considerably higher than the threshold value of 25, proposed by Raudkivi and Ettema [11], to diminish the effect of sediment size on scour depth. Also, according to Breusers and Raudkivi (1991), the median grain size of the bed material was larger than 0.7 mm to preserve the formation of ripples. The inlet flow was measured by means of a calibrated magnetic flow meter with an accuracy of ±1 l/s within the range of the experimental discharges. Furthermore, the depth of flow as well as the depth of scour was measured using a Luminometers with a resolution of ±0.1 mm. the device was mounted on a carriage installed above the flume walls which provided longitudinal and transverse movement of the instrument. At the end of the flume an adjustable tail gate was installed which provided different depths of flow over the sediment recess. Total 35 experiments were carried out. Several researchers have studied time-dependent scour depth for clear water condition. They have come up with different definitions of time to reach the equilibrium scour depth. In clear water condition the equilibrium scour depth is reached asymptotically with the time [12, 13]. Kumar et al. [14] stopped their experiments when the scour depth did not change by more the 1 mm over a period of 3 h. Mia and Nago [15] stopped their experiments when there was less than 1 mm change in scour by 1 h. Yanmaz and Altinblink [16] and Mia and Nago [15] have indicated that most of the scour occurs during the first 3 or 4 h of experiment. Melville and Chiew [12] defined the equilibrium time when the scour depth did not change by more than 5% of the pier diameter over a period of 24 h, and suggested the following equation for predicting the equilibrium time in the clear water condition:

$$\frac{d_s}{d_{se}} = \exp\left\{-0.03\left|\frac{u}{U_c}\ln\frac{t}{t_c}\right|^{1/6}\right\} \tag{17.1}$$

In which d_s is the scour depth, d_{se} is the equilibrium scour depth, u is the local velocity, U_c is the critical velocity, t is the time, and t_e is the equilibrium time.

In this study, a long time experiment was carried out for 50 h according to the criteria of [12]. The results indicate that, depth of scour increases with the time and there is a good agreement between experimental data and equation (time equilibrium) for the equilibrium time. It was found that 36 h was necessary for reaching equilibrium scour depth, and it was observed that 90% equilibrium scour depth occurred in 1/3 equilibrium time. In the present study, the time duration of the tests is limited to 180 min in which more than 80% of equilibrium scour depth occurred. Table 17.1 shows the initial conditions implemented in different runs.

17.2.1 Clear Water Calculations

Before starting the main experiments, a series of tests were conducted to determine the threshold of particle motion. For this purpose, two separate methods were implemented. In the first method, the inception of particle motion was determined by means of the shield's diagram. for the values of $d_{50} = 0.8$ mm, $\upsilon = 10^{-6}$ m^2/s and s = 2.65, where υ and s are respectively the kinematic viscosity of water and the sediment to water specific weight ratio, the corresponding shields' parameter yields; $\tau^* = 28.8$. The critical shear stress, τ_c, is calculated from the shields' parameter expression:

$$\tau^* = \frac{\tau_c}{\rho g(s-1)d_{50}} \tag{17.2}$$

Further the allowable shear stress was conservatively limited to $0.9\tau_c$, which was $0.9 \times 0.41 = 0.37$ N/m^2. Then for various depths of flow and discharges the bed shear stress was obtained from Eq. 17.3:

$$\tau = \rho g y s_0 \tag{17.3}$$

where y is the depth of flow and s_0 is the slope of energy line.

Finally, by comparison of the allowable shear stress and the critical shear stress it is decided whether the clear water condition is dominated or the live bed state. The summary of the calculations is presented in Table 17.2.

In the second method the critical shear velocity, u^*_c, is obtained from Eq. (17.4) and the shields' diagram.

$$R_c = \frac{u_c^* d_{50}}{\upsilon} \tag{17.4}$$

where R_c is the critical Reynolds number determined from the Shields' diagram. The critical shear velocity corresponding to current experiments was 0.018 m/s. Then the critical mean flow velocity, U_c, was determined from the following logarithmic

Table 17.1 Summary of the initial conditions

Run no	Pier condition	Plates configuration	Lateral plates (cm)	Middle plate (cm)	Test duration (min)	Discharge (L/s)	Flow depth (cm)
1	Without plates	–	–	–	180	15	8
2	Without plates	–	–	–	180	22	11
3	Without plates	–	–	–	180	25	12
4	Without plates	–	–	–	180	35	15
5	Without plates	–	–	–	180	45	18
6	Protected	Type 1	8 * 12	12 *12	180	15	8
7	Protected	Type 1	8 * 12	12 *12	180	22	11
8	Protected	Type 1	8 * 12	12 *12	180	25	12
9	Protected	Type 1	8 * 12	12 *12	180	35	15
10	Protected	Type 1	8 * 12	12 *12	180	45	18
11	Protected	Type 2	8 * 12	12 *12	180	15	8
12	Protected	Type 2	8 * 12	12 *12	180	22	11
13	Protected	Type 2	8 * 12	12 *12	180	25	12
14	Protected	Type 2	8 * 12	12 *12	180	35	15
15	Protected	Type 2	8 * 12	12 *12	180	15	18
16	Protected	Type 3	8 * 12	12 *12	180	15	8
17	Protected	Type 3	8 * 12	12 *12	180	22	11
18	Protected	Type 3	8 * 12	12 *12	180	25	12
19	Protected	Type 3	8 * 12	12 *12	180	35	15
20	Protected	Type 3	8 * 12	12 *12	180	45	18
21	Protected	Type 1	14 * 12	12 *12	180	15	8
22	Protected	Type 1	14 * 12	12 *12	180	22	11
23	Protected	Type 1	14 * 12	12 *12	180	25	12
24	Protected	Type 1	14 * 12	12 *12	180	35	15
25	Protected	Type 1	14 * 12	12 *12	180	45	18
26	Protected	Type 2	14 * 12	12 *12	180	15	8
27	Protected	Type 2	14 * 12	12 *12	180	22	11
28	Protected	Type 2	14 * 12	12 *12	180	25	12
29	Protected	Type 2	14 * 12	12 *12	180	35	15
30	Protected	Type 2	14 * 12	12 *12	180	45	18
31	Protected	Type 3	14 * 12	12 *12	180	15	8

(continued)

Table 17.1 (continued)

Run no	Pier condition	Plates configuration	Lateral plates (cm)	Middle plate (cm)	Test duration (min)	Discharge (L/s)	Flow depth (cm)
32	Protected	Type 3	14 * 12	12 *12	180	22	11
33	Protected	Type 3	14 * 12	12 *12	180	25	12
34	Protected	Type 3	14 * 12	12 *12	180	35	15
35	Protected	Type 3	14 * 12	12 *12	180	45	18

Table 17.2 Clear water flow manipulation

Depth of flow (cm)	Flow discharge (L/s)	U (m/s)	Bed induced shear stress, τ (Pa)	$\frac{\tau}{\tau_c}$	U_c	$\frac{U}{U_c}$
18	45	0.31	0.35	0.94	0.33	0.93
15	35	0.29	0.29	0.78	0.32	0.89
12	25	0.26	0.23	0.63	0.32	0.82
11	22	0.25	0.21	0.58	0.31	0.80
8	15	0.23	0.15	0.42	0.29	0.79

equation; [17].

$$\frac{U_c}{u*_c} = 5.75 \log\left(\frac{y}{2d_{50}}\right) + 6 \tag{17.5}$$

The ratio U/U_c, where U is the mean flow velocity is determined. For the values of U/U_c smaller than unity, the clear water condition prevails. The results of the computational efforts are inserted in Table 17.2. Besides, the results obtained from aforementioned approaches were verified by observations and monitoring the bed profile variations at equal time intervals.

17.3 Results

17.3.1 Equilibrium Scour Test

Tests on scour at the pier were carried out in three stages: (1) a long term scour evaluation test for single pier without the plates and the three aforementioned plates' configurations of the current study was performed to determine the equilibrium scour depth. (2) short term scour tests (180 min) on pier without plates for three different discharges of this study were done (3) short term scour tests on pier with plates in place, according to the three suggested arrangements of the paper. Figure 17.2 shows

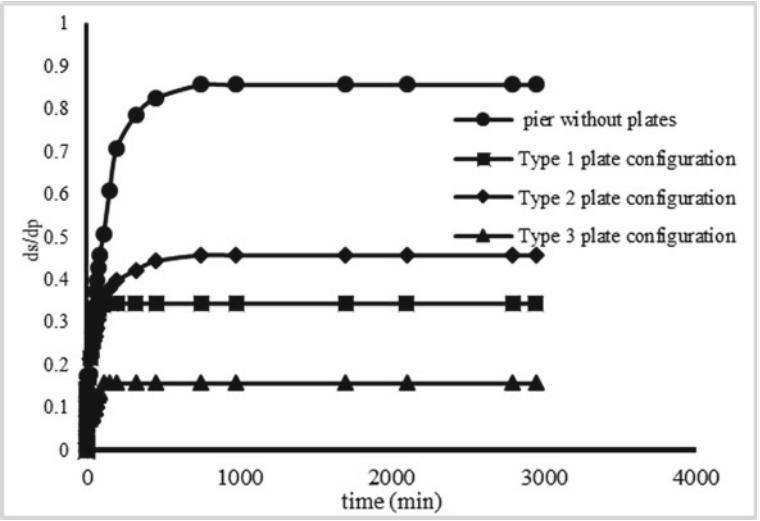

Fig. 17.2 Variation of the maximum scour depth (non-dimensional parameter) versus time

the development of the time dependent scour depth in single pier as well as the three countermeasure types implemented in current study. As seen the trend line of the variations are similar. Comparison of the curves for type 1 plate configuration and type 2 plate configuration (upstream plate versus downstream plate configuration) reveals that installation of the plate at the pier nose is more effective in preserving the pier against scour.

17.3.2 Scour Pattern

In the first series of the tests the plates were installed at the upstream face of the pier. The length of the lateral plates was 8 cm. The middle plate was effective in reducing the strength of the downward flow by dividing it into two branches. These two downward jets produce two small slots at the pier nose. Then small vertical structures form in these slots which commence in transferring particles toward upstream and digging a hole at the vicinity of the pier nose. Simultaneously the scour occurs along the plates. The particles moving between the two lateral plates partially fill the scour hole at the pier nose. The two lateral plates act as bed armoring countermeasure and confine the motion of the particles. Based on scouring pattern 8 separate zones are identified around the pier. These zones are shown in Fig. 17.3. As seen zone 1 forms upstream of the lateral plates' edges. Small vortices in this zone are the major sources of scour in this zone. Part of the scoured particles is transferred along the outer side of the lateral plates which deposit gradually in zones 2 and 3. The slope of the deposited particles in zone 3 is larger than that of zone 2. In zone 4, the scour pattern, similar to

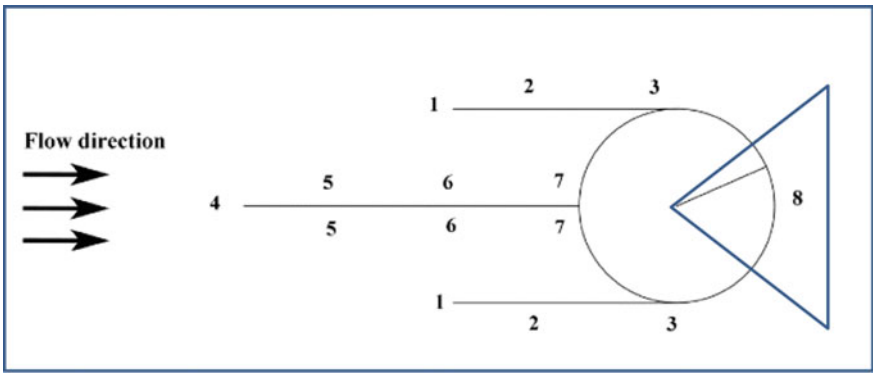

Fig. 17.3 Different scour and deposition zones (plate configuration-type 1)

zone 1but with smaller scour hole is observed. In zone 6 the interaction of the vortices at the pier nose and the approaching flow is seen. The vortices at the pier nose carry sediment in upstream direction while the approaching flow transfers sediment from zone 4 and 5. Interference of the two opposite streams generates a hill of deposited materials in zone 6. Figure 17.4 shows the trace of sediments along the middle plate. As it is observed the slope of the bed profile near the pier is smaller. Finally, the scoured particles which are carried along the outer face of the lateral plates pile up at the pier rear in zone 8.

Experiments on the performance of plates attached to the downstream face of the pier revealed that the plate were not remarkably effective in mitigating the scour depth at the upstream face. It was also observed that inserting the plates at the downstream pier face increases the volume of deposited sediment at the pier rear. The scour pattern at the pier nose was similar to the single pier without any protective plates.

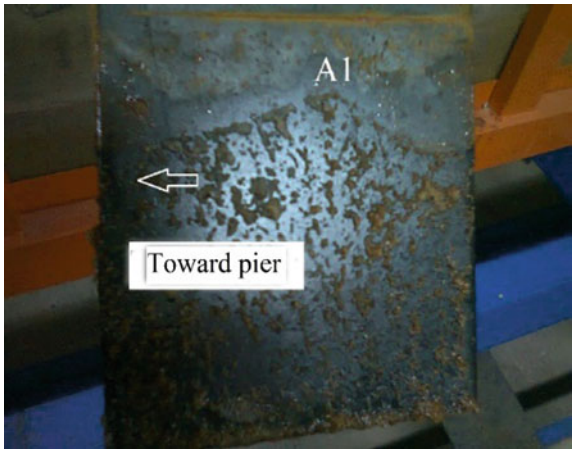

Fig. 17.4 Scour profile along the middle plate

Fig. 17.5 Deposition zone (zone 8) in type 2 plate configuration

Figure 17.5 shows a photo of the deposition zone (zone8) between the type 2 plates configuration.

It is seen that implementation of type 3 plate configuration is highly efficient in scour control around the pier. For the upstream face the same zonation areas of the type 1 plate setup exists. Furthermore, downstream plates protect the pier from the lee- wake effects.

17.3.3 Quantitative Results

Figure 17.6 shows the scour and deposition contours in (a) single pier without any scour countermeasure (b) pier with type 1 plate countermeasure (c) pier with type 2 plate countermeasure and (d) pier with type 3 plate countermeasure for the maximum discharge of 45 L/s. As observed, the scour geometry in type 3 plate configuration is comparatively smaller than the other cases. Also it is seen that the maximum scour depths for all cases occur at the pier nose. Meanwhile it is found that the maximum scour depth in type3 plate configuration is the smallest. The ratio of scour area for each type of configurations used in current study to the scour area around single pier without any countermeasure indicates the efficacy of the setup. This ratio for type 1 plate countermeasure is 47.5%, for type 2 is 7% and for type 3 is 62% which confirms the superiority of the type 3 configuration in comparison to type 2 and 1 configuration.

Figure 17.7 compares respectively the longitudinal scour profiles along the pier center line for type 1, type 2 and type 3 plate configuration as well as single pier without any plates, under the maximum discharge of 45 L/s. It is evident that the length of the scour and deposition zone in type 2 Plate configuration is smaller than

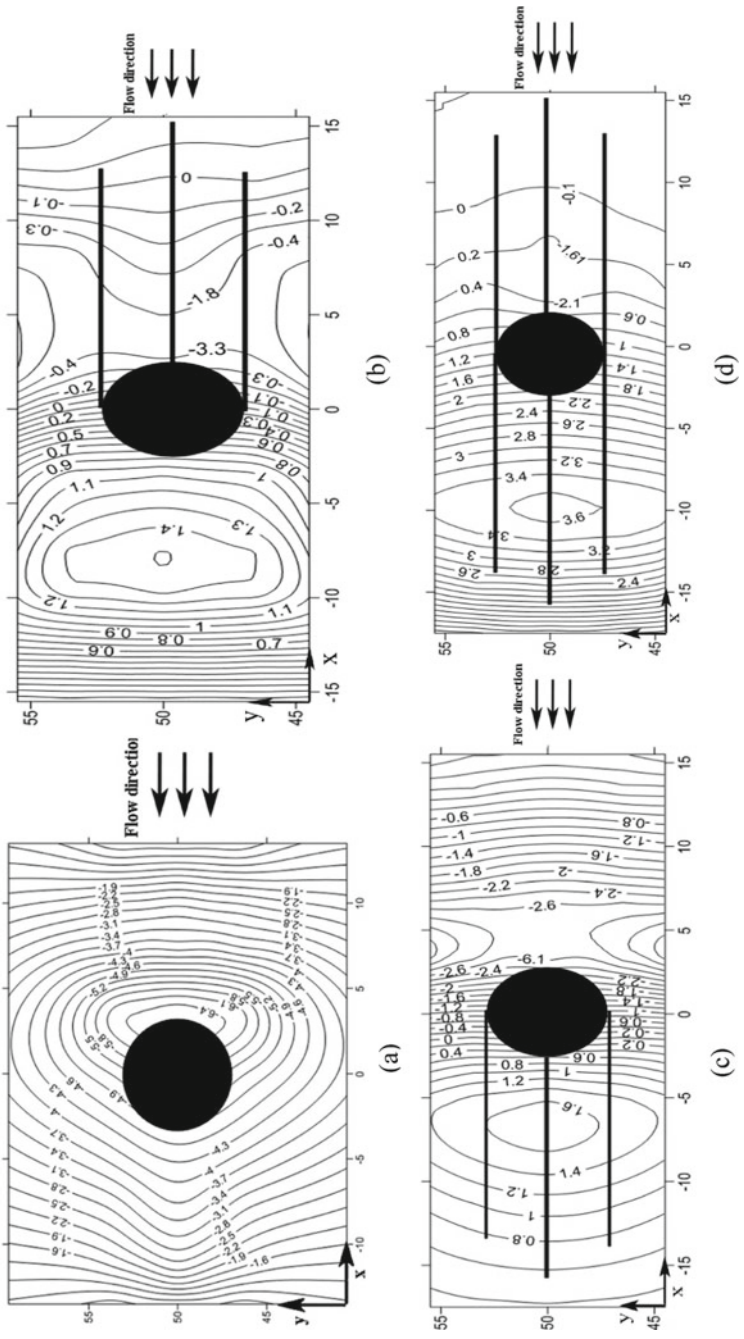

Fig. 17.6 Comparison of scour and deposition contours in **a** single pier, **b** pier with type 1 plate configuration, **c** pier with type 2 plate configuration, **d** pier with type 3 plate configuration (Q = 45 L/s)

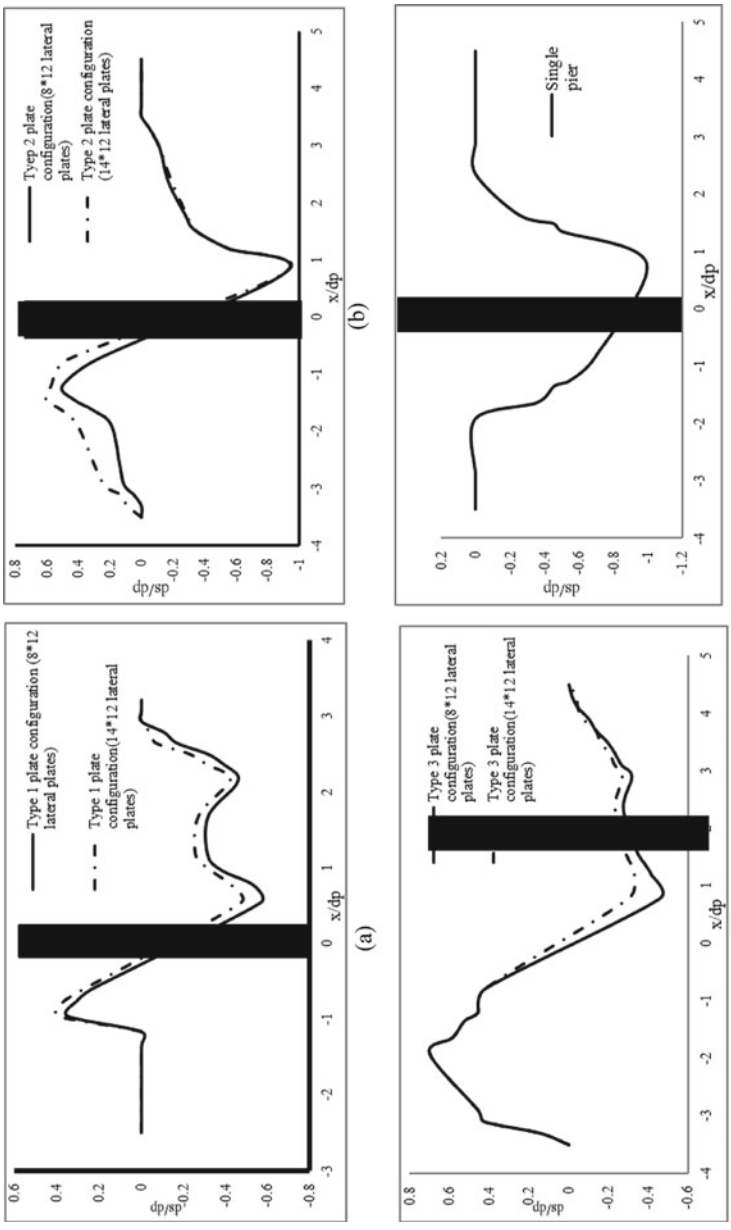

Fig. 17.7 Longitudinal scour profiles: **a** pier with type 1 plate configuration, **b** pier with type 2 plate configuration, **c** pier with type 3 plate configuration, **d** single pier (Q = 45 L/s)

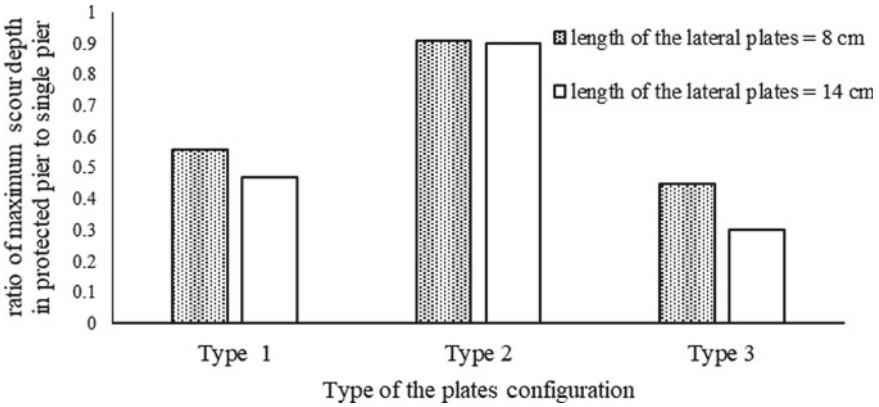

Fig. 17.8 Variation of maximum scour depth in different cases

the others. Also it is interesting to note that the maximum deposition height is formed in type 3 plate configuration.

Figure 17.8 shows the variation of the ratio of maximum scour depth for different configurations to the maximum scour depth in single pier without plates for the maximum discharge of 45 L/s. The results show that the maximum efficiency in scour reduction is 62% for type 3 plate configurations. Type 1 and type 2 plate configurations provide efficiencies of 47.5 and 7% respectively. Also it is found that longer plates increase the plates efficiency by 20% in type 1 and type 3 configuration.

17.4 Conclusion

The results of experiments indicate that triple rectangular plates as local scour countermeasure have various impacts on the bottom elevation. In addition, results show that triple rectangular plates act as either flow altering and bed armoring simultaneously. On the basis of qualitative results, type 2 and type 3 plates configuration have the lowest and highest impact on local scour reduction respectively. The type 3 configuration has maximum efficiency in scour reduction roughly 62%, whereas type 2 configuration only brings 9% protective effects. Furthermore, it could be interpreted from qualitative results, the range of bottom erosion reduces when the length of lateral plates increase. The impact of longer lateral plates on bottom scour protection is about 20%, when type 3 configuration is implemented.

References

1. Kandasamy JK, Melville BW (1998) Maximum local scour depth at bridge piers and abutments. J Hydraul Res 36(2):183–197
2. Chabert J, Engeldinger P (1956) Etude des affouilements autour des piles des ponts. Study on scour around bridge piers, Laboratoire National d'Hydraulique, Chatou, France (in French)
3. PARKER G, TORO-ESCOBAR C and VOIGT RL (1998) Countermeasures to Protect Bridge Piers from Scour. National Highway Research Program, Transportation Research Board, National Research Council, University of Minnesota, Minneapolis, Final Report.Pier Scour Countermeasures. Department of Civil and Resource Engineering
4. Ghorbani B, Kells JA (2008) Effect of submerged vanes on the scour occurring at a cylindrical pier. Hydraul Res J 46(5):610–619
5. Maza Alvarez JA, Echavarria Alfaro FJ (1973) "Contribution to the study of general scour." Proc., Int. Symp. on River Mech., IAHR, Bangkok, Thailand, 795–803
6. Gupta AK, Gangadharaiah T (1992) Local scour reduction by a delta wing-lick passive device. Proc., 8th Congr. of Asia and Pacific Reg. Div., 2, CWPRS, Pune, India, B471–B481
7. Daido A (1993) Plotection of Local Scour around Piers with Guide Wall and Slanting Plate attached Piers Surface. PROCEEDINGS OF HYDRAULIC ENGINEERING. 37:529–536. https://doi.org/10.2208/prohe.37.529
8. Odgaard AJ, Wang Y (1991) "Sediment management with submerged vanes, I: Theory" J Hydraul Eng, 117(3):267–283
9. Lauchlan CS (1999) "Pier scour countermeasures."Ph.D. thesis, Univ. of Auckland, Auckland, New Zealand
10. Chiew YM, Melville BW (1987) Local scour around bridge piers. J Hydraul Res 25(1):15–26
11. Raudkivi A, Ettema R (1983) Clear water scour at cylindrical piers. J Hydraul Eng 109(3):338–350
12. Melville BW, Chiew YM (1999) Time scale for local scour at bridge piers. J Hydraul Eng 125(1):59–65
13. Breusers HNC, Nicollet G, Shen HW (1977) Local scour around cylindrical piers. J Hydraul Resour IAHR 15(3):211–252
14. Kumar V, Raju KGR, Vittal N (1999) Reduction of local scour around bridge piers using slots and collars. J hydraul eng-asce. 125, https://doi.org/10.1061/(ASCE)0733-9429(1999)125:12(1302)
15. Mia MdF, Nago H (2003) Design method of time-dependent local scour at a circular bridge pier. J Hydraul Eng 129(6):420–427
16. Yanmaz AM, Altinbilek HD (1991) Study of time-dependent local scour around bridge piers. J Hydraul Eng 117(10):1247–1268
17. Chiew YM (1995) Mechanics of riprap failure at bridge piers. J hydraul eng-asce. 121, https://doi.org/10.1061/(ASCE)0733-9429(1995)121:9(635)
18. Tafarojnoruz A, Gaudio R, Calomino F (2012) Evaluation of flow-altering countermeasures against bridge pier scour. J Hydraul Eng. 138:297–305. https://doi.org/10.1061/(ASCE)HY.1943-7900.0000512